

Supplementary information

DNA-catalyzed alternative RNA splicing

Dongying Wei,^a Mingmei Gao,^a Jiajie Guo,^a Yueyao Wang,^a Xintong Li,^b Zhe Li^{*c} and Hanyang Yu^{*a}

^a State Key Laboratory of Coordination Chemistry, Department of Biomedical Engineering, College of Engineering and Applied Sciences, Chemistry and Biomedicine Innovation Center (ChemBIC), Jiangsu Key Laboratory of Artificial Functional Materials, Nanjing University, Nanjing, Jiangsu 210023, China.

^b Department of Oncology, The First Affiliated Hospital of Nanjing Medical University, Nanjing, Jiangsu 210023, China.

^c State Key Laboratory of Analytical Chemistry for Life Science, Department of Biomedical Engineering, College of Engineering and Applied Sciences, Nanjing University, Nanjing, Jiangsu 210023, China.

* Corresponding authors: Zhe Li and Hanyang Yu

Zhe Li: zheli@nju.edu.cn

Hanyang Yu: hanyangyu@nju.edu.cn

Experimental section

Chemicals and materials. DNA oligonucleotides and short RNA oligoribonucleotides were purchased from Sangon Biotech (Shanghai, China) and GenScript (Nanjing, China). Long RNA oligoribonucleotides were prepared either by ligation of two short RNA fragments using T4 RNA ligase 1 (New England Biolabs) or by a primer extension reaction of a Cy5-labeled RNA primer on a DNA template (Table S1) in the presence of NTPs and TGK polymerase,¹ and purified by denaturing polyacrylamide gel electrophoresis (PAGE). The expression plasmid of TGK polymerase [TgoT (E664K, Y409G)] is obtained by first fusing the existing D4K polymerase plasmid pQE-80L-D4K [TgoT (L403P, P657T, E658Q, K659H, Y663H, E664K, D669A, K671N, T676I)] and RT521K polymerase plasmid pQE-80L-RT521K [TgoT (A385V, E429G, F445L, I521L, E664K, K726R)] in the laboratory to obtain pQE-80L-TgoT (L403P, E664K, K726R) plasmids, followed by three point mutagenesis to revert L403P and K726R and to install Y409G. TGK polymerase was expressed from BL21(DE3) expressing competent cells and purified by Ni-NTA resins. All the nucleic acid samples were dissolved in ultrapure water at room temperature and quantified on NanoDrop.

DFHBI-1T was purchased from Sigma-aldrich (Shanghai, China). 2,2'-azino-bis(3-ethylbenzothiazoline-6-sulfonic acid) diammonium salt (ABTS) was purchased from TCI Shanghai. H₂O₂ (30% v/v) was purchased from Aladdin (Shanghai, China). Hemin was purchased from MedChemExpress (Shanghai, China). All the buffers were prepared using ultrapure water purified by a Millipore filtration system.

Truncation analysis of deoxyribozyme 7CX10. 100 nM Cy5.5-labeled left RNA substrate (with a 2',3'-cyclic phosphate group, obtained from the cleavage reaction catalyzed by deoxyribozyme 8-17), 1 μM right RNA substrate (with a 5'-hydroxyl group) and 400 nM deoxyribozyme 7CX10 variant were mixed in a reaction buffer (70 mM Tris, 150 mM NaCl, 2 mM KCl, and 1 mM ZnCl₂, pH 7.5), and then incubated at 23°C for 3 h. Reactions were stopped by adding 30 μL stop buffer (8 M urea in 1× TBE), analyzed by 20% denaturing PAGE, and visualized on a LI-COR Odyssey CLx imaging system.

Optimization of the cleavage and ligation reaction conditions. The cleavage reactions contained 100 nM Cy5.5-labeled RNA substrate, 1 μM deoxyribozyme 8-17 in a buffer (70 mM Tris, 150 mM NaCl, 2 mM KCl, pH 7.5). The sample was annealed by heating at 95°C for 2 min and cooling to room temperature for over 15 min.² ZnCl₂ (final concentration 1 mM) was added to initiate the reaction. The reaction was incubated at 23°C for 30 min, quenched by addition of 30 μL stop buffer, and analyzed by 20% denaturing PAGE. The deoxyribozyme:substrate ratio varied (1:1, 2:1, 5:1 and 10:1). The Zn²⁺ concentration varied (0.1, 0.5 and 1.0 mM). The reaction time varied (15, 30 and 60 min). Two different buffers were tested (Buffer 1: 50 mM Tris, 1 mM ZnCl₂ and 1 M NaCl at pH 7.5. Buffer 2: 70 mM Tris, 1 mM ZnCl₂, 150 mM NaCl and 2 mM KCl at pH 7.5). Reactions with and without annealing were also tested.

The ligation reaction contained 100 nM Cy5.5-labeled left RNA substrate with a 2',3'-cyclic

phosphate group, 1 μM right RNA substrate with a 5'-hydroxyl group and 400 nM deoxyribozyme 7CX10t in a buffer (70 mM Tris, 1 mM ZnCl_2 , 150 mM NaCl and 2 mM KCl at pH 7.5). The reaction was incubated at 23°C for 3 h, quenched by addition of stop buffer, and analyzed by 20% denaturing PAGE.³ Reactions under different conditions were tested, including temperature (23 and 37°C), with and without annealing, and divalent metal ion (Zn^{2+} , Mn^{2+} , Ba^{2+} , Cu^{2+} , Sr^{2+} , Mg^{2+} , Ca^{2+} , Ni^{2+} , Co^{2+}). The final concentration of the divalent metal ion was 10 mM except for Zn^{2+} (1 mM) and Mn^{2+} (1 mM).

Ligation site requirement of 7CX10t. Four RNA fragments differing in the last residue, which would be used as left substrate in subsequent ligation reactions, were first prepared by deoxyribozyme 8-17-catalyzed cleavage reactions. Four RNAs (RNA substrate-A, RNA substrate-G, RNA substrate-C and RNA substrate-U) were separately cleaved by a universal deoxyribozyme 8-17 (Table S3) at a specific cleavage site NG (AG, GG, CG, UG)⁴. The cleavage reactions contained 1 μM Cy5-labeled RNA substrate, 10 μM deoxyribozyme 8-17 in a buffer (70 mM Tris, 150 mM NaCl, 2 mM KCl, pH 7.5). The sample was annealed by heating at 95°C for 2 min and cooling to room temperature for over 15 min. ZnCl_2 (final concentration 1 mM) was added to initiate the reaction. The reaction was incubated at 37°C for different time (3 h for RNA substrate-A, RNA substrate-G and RNA substrate-U; 12 h for RNA substrate-C). The 5' cleavage product was recovered by gel purification. Four right RNA substrates with 5'-hydroxyl group were prepared by solid-phase synthesis (RNA substrate-A, RNA substrate-G, RNA substrate-C and RNA substrate-U in Table S3).

The ligation reaction contained 100 nM Cy5-labeled left RNA substrate with a 2',3'-cyclic phosphate group, 1 μM right RNA substrate with a 5'-hydroxyl group and 400 nM deoxyribozyme 7CX10t in a buffer (70 mM Tris, 1 mM ZnCl_2 , 150 mM NaCl and 2 mM KCl at pH 7.5). The reaction was incubated at 23°C for 3 h, quenched by addition of stop buffer, and analyzed by 12% denaturing PAGE. Both the original 7CX10t and a variant with compensatory mutations were tested for each substrate combination.

Splicing and alternative splicing of the model RNA. First, in the cleavage reaction, 100 nM Cy5.5-labeled precursor RNA was cleaved by deoxyribozyme variants 8-17-1 and 8-17-2 at 23°C for 30 min, and analyzed by denaturing PAGE. The amount of the 5' cleavage product (exon 1) was calculated. Subsequently, in the splicing reaction, precursor RNA was first cleaved by 8-17-1 and 8-17-2. Then nine equivalents of right RNA substrate (exon 2) and four equivalents of deoxyribozyme 7CX10t-1 were added and incubated at 23°C for 3 hours. The reaction was quenched by addition of 30 μL stop buffer, and analyzed by 12% denaturing PAGE.

For the alternative splicing reaction, the precursor RNA was first prepared by T4 RNA ligase reaction. The ligation reaction contained Cy5.5-labeled left RNA fragment with a 3'-hydroxyl group (2.5 μM), right RNA fragment with a 5'-monophosphate group (10 μM), a DNA splint sequence (10 μM), 1 mM ATP and 500 U/mL T4 RNA ligase in a reaction buffer (50 mM Tris-HCl at pH 7.5, 10 mM MgCl_2 , 1 mM DTT). The two RNA fragments and the DNA splint were first annealed by heating at 95°C for 2 min and then cooling to 23°C for 15

min. T4 RNA ligase was then added to initiate the reaction. The reaction was incubated at 25°C for 3 h. The ligation product was analyzed and recovered by 12% PAGE.

The alternative splicing reaction was performed similarly. The precursor RNA was first cleaved by deoxyribozyme 8-17 variants. Then nine equivalents of right RNA substrate and four equivalents of deoxyribozyme 7CX10t variant were added to initiate the ligation reaction. The products were analyzed by 12% denaturing PAGE.

Splicing and circular dichroism of RNA G-quadruplex. A precursor RNA sequence was first designed such that after removal of the “intron”, the splicing product was predicted to form a G quadruplex structure, while before splicing the precursor was predicted to form a hairpin structure. The structural prediction was performed using RNAstructure and Quadruplex forming G-Rich Sequences (QGRS) Mapper software (<https://bioinformatics.ramapo.edu/QGRS/index.php>).

The splicing reaction was performed similarly with the appropriate deoxyribozyme 8-17 and 7CX10t variants, and the product was analyzed and recovered by 12% denaturing PAGE. In order to verify the formation of the predicted structure, the circular dichroism spectra of the precursor RNA and splicing product were analyzed on a Jasco J-810 spectropolarimeter. A chemically synthesized RNA with the identical sequence to the splicing product was used as a control.

Splicing and activity test of hammerhead ribozyme. A hammerhead ribozyme variant sequence was first designed such that it contained a UAGG tetranucleotide region, a potential ligation site of deoxyribozyme 7CX10t. This variant substituted two G:C base pairs in the wild-type sequence by one C:G pair and one U:A pair. The self-cleavage activities of the hammerhead ribozyme wild-type and variant were tested by incubating 100 nM ribozyme in a reaction buffer containing 50 mM Tris (pH 7.0), 10 mM Mg²⁺ or 1 mM Zn²⁺ at 23°C for 10 min.

Precursor RNA sequences were then designed with the hope that the addition of an “intron” sequence would, at least partially, disrupt the correct folding and thus affect the catalytic activity of the ribozyme. The precursor RNA sequences were first prepared by T4 RNA ligase reaction. The ligation reaction contained a left RNA fragment with a 3'-hydroxyl group (10 μM), a right RNA fragment with a 5'-monophosphate group and a 3' Cy5.5 modification (2.5 μM), a DNA splint sequence (10 μM), 1 mM ATP and 500 U/mL T4 RNA ligase in a reaction buffer (50 mM Tris-HCl at pH 7.5, 10 mM MgCl₂, 1 mM DTT). The two RNA fragments and the DNA splint were first annealed by heating at 95°C for 2 min and then cooling to 23°C for 15 min. T4 RNA ligase was then added to initiate the reaction. The reaction was incubated at 25°C for 3 h. The ligation product was analyzed and recovered by 12% PAGE.

The splicing reaction was performed similarly with the appropriate deoxyribozyme 8-17 and 7CX10t variants, and the product was analyzed and recovered by 12% denaturing PAGE. The

kinetics of the self-cleavage reactions catalyzed by the precursor and the splicing product were determined in the reaction buffer containing 50 mM Tris (pH 7.0), 10 mM Mg²⁺ at 23°C. For precursor, at specific time points (0, 0.33, 0.67, 1, 1.5, 2, 3, 4, 5, 6, 8, 10 min), the reaction was quenched and analyzed on denaturing PAGE. For the splicing product, at specific time points (0, 0.25, 0.33, 0.67, 1, 1.5, 2, 3, 4, 5 min), the reaction was quenched and analyzed on denaturing PAGE. k_{obs} was calculated by fitting the product percentage and reaction time to the following first-order reaction kinetics equation using Prism 7.0a.

$$Y = Y_{\text{max}} * (1 - e^{-kt})$$

where Y is the self-cleaved product percentage at time t, Y_{max} is the apparent maximum self-cleaved product percentage, and k is the observed first-order reaction rate constant.

The splicing product (i.e. mature hammerhead ribozyme) could not undergo spontaneous self-cleavage reaction immediately after the splicing reaction, because the ligase deoxyribozyme 7CX10t was still bound and prevented the correct intramolecular folding of the mature hammerhead. Only after gel purification to remove 7CX10t could the catalytic activity of the splicing product be tested.

Sequencing of spliced products. The purified spliced product was reverse transcribed into cDNA, using the extended RT primer 1 for G-quadruplex and the extended RT primer 2 for hammerhead ribozyme variant to add a binding region for subsequent PCR reaction. 10 pmol of the spliced product was mixed together with 11 pmol of RT primer in water, annealed by heating at 65°C for 5 min and incubating on ice for 3 min. After 2 μ L 5 \times Hifair II Buffer Plus and 1 μ L Hifair II Enzyme Mix was added, the 10 μ L reaction was incubated at 25°C for 5 min, then at 42°C for 10 min, finally at 85°C for 5 min. The reverse transcription products were used as templates in the following PCR reactions. Primers G-Primer 2/3 for G-quadruplex and H-Primer 2/3 for hammerhead ribozyme variant were used. The generated dsDNA strands were cloned into pEASY-T1 vectors and sent for Sanger sequencing⁵.

Production of isoforms with different activities via alternative splicing. A precursor RNA that contained two functional motifs (Broccoli aptamer and G quadruplex with peroxidase activity) was designed and prepared by primer extension. The sequences of the two functional motifs were not continuous and interrupted by an intentionally inserted intron. The primer extension reaction contained 1 μ M RNA primer, 1 μ M DNA template, 0.625 mM NTPs each and 0.05 mg/mL TGK polymerase in a buffer [20 mM Tris-HCl, 10 mM (NH₄)₂SO₄, 10 mM KCl, 2 mM MgSO₄, 0.1% Triton X 100, 3 mM MgSO₄, pH 8.8]. The primer-template complex was first annealed by heating at 94°C for 30 sec, cooling to 4°C for 15 min and on ice for 3 min. TGK polymerase was added to initiate the reaction, and the reaction was incubated at 65°C for 30 min. After the primer extension reaction, 1 U/mL DNase I was added and incubated at 37°C for 2 h to digest the DNA template. The RNA product was analyzed and recovered by 12% PAGE.

The alternative splicing reactions were performed similarly with the appropriate deoxyribozyme 8-17 and 7CX10t variants, and the products were analyzed and recovered by 12% denaturing PAGE.

In order to evaluate the peroxidase activity, RNAs (0.25 μM) were annealed by first heating at 70°C for 5 min and then cooling on ice for 2 h. The annealed RNAs were incubated with hemin (0.25 μM) in MES buffer (25 mM MES, 200 mM NaCl, 10 mM KCl, 1% DMSO, 0.05% Triton X-100, pH 5.1) at 25°C for 0.5 h. After the formation of RNA–hemin complex, ABTS (0.5 mM) and H₂O₂ (0.5 mM) were added to the solution and incubated at 25°C for 4 h. After the reaction, the absorbance at 415 nm was recorded on a Nanodrop 2000 spectrophotometer.⁶

In order to evaluate the fluorescence-promoting activity, RNAs (1.5 μM) and DFHBI-1T (15 μM) were mixed in a buffer (100 mM KCl, 1 mM MgCl₂, 40 mM HEPES, pH 7.4), and then incubated at 25°C for 90 min. The fluorescence intensities (excitation: 460 nm; emission: 500 nm) were collected on a MD SpectraMax iD5 microplate reader.⁷

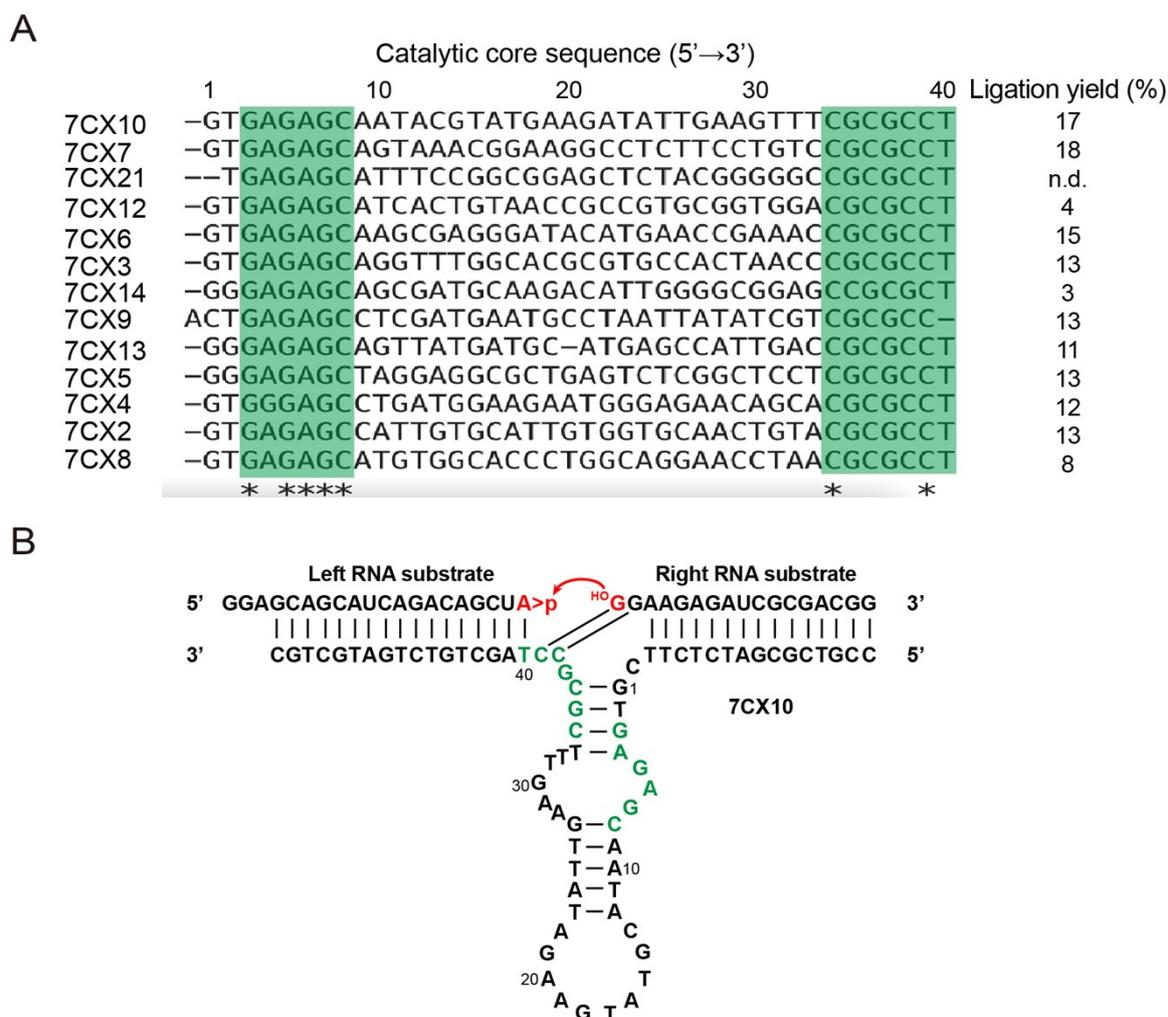


Figure S1. Alignment of 7CX family sequences and predicted secondary structure of 7CX10-0 and with RNA substrates. (A) 7CX family sequences were aligned using Clustal Omega and two conserved regions were highlighted in green. The ligation reactions were performed in a reaction buffer containing 70 mM Tris (pH 7.5), 1 mM ZnCl₂, 150 mM NaCl and 2 mM KCl at 23°C for 3 h. [Left RNA substrate] = 100 nM. [Right RNA substrate] = 1,000 nM. [Enzyme] = 400 nM. (B) The secondary structure of deoxyribozyme 7CX10 and the RNA substrates was predicted by RNAstructure. The deoxyribozyme 7CX10 catalyzed an RNA ligation reaction between a left substrate with a terminal 2',3'-cyclic phosphate and a right substrate with a 5'-hydroxyl group. The two nucleotides at the ligation junction were shown in red. The conserved residues within deoxyribozyme catalytic core were shown in green.

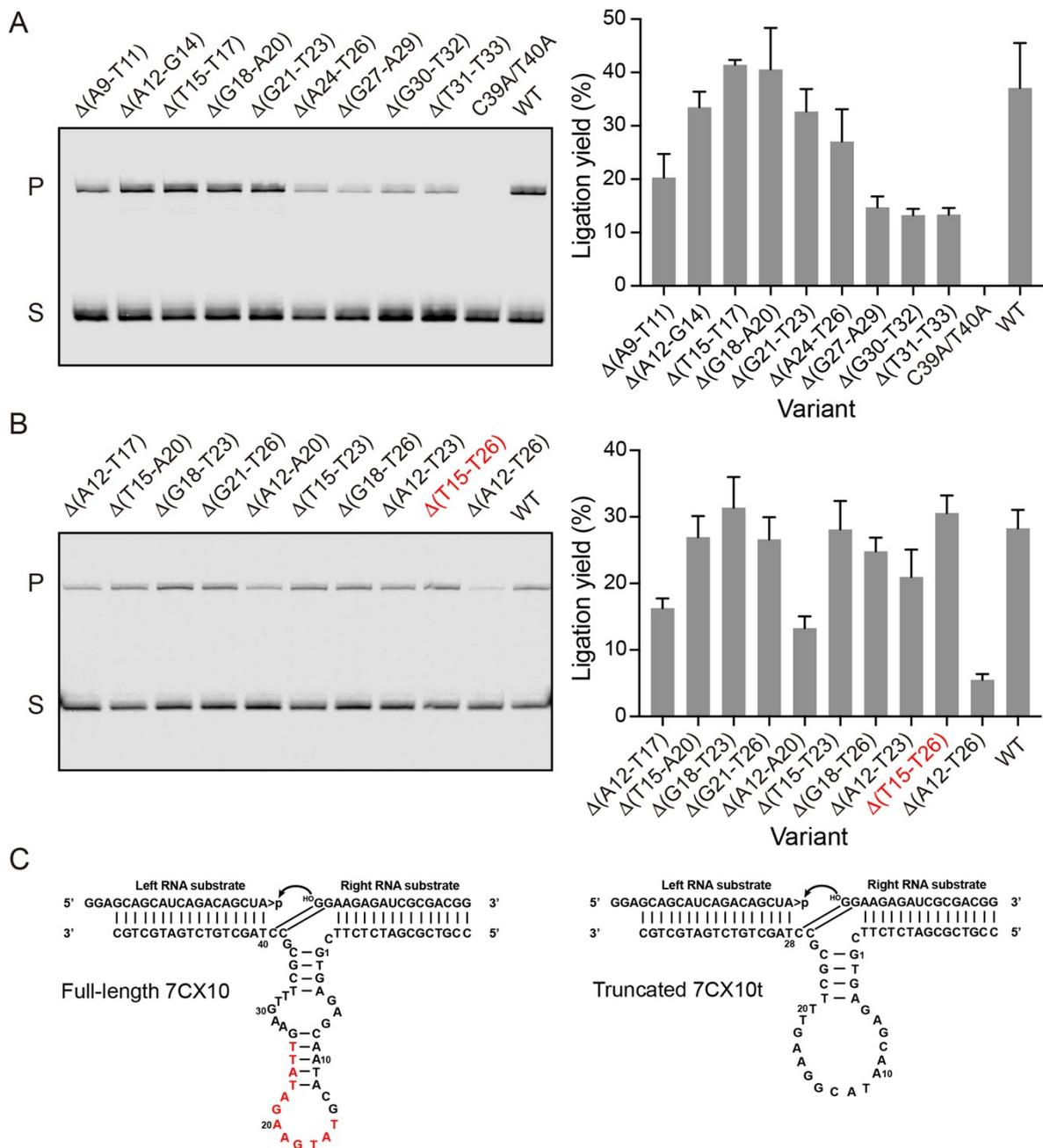


Figure S2. Truncation analysis of deoxyribozyme 7CX10 catalytic core. (A) Each truncation variant contained a deletion of three nucleotides in the non-conserved region compared with the full-length wild-type (WT). Variant C39A/T40A contained two substitutions. The results showed that residues from A12 to T26 seemed dispensable, whereas C39 and T40 were essential and likely formed base pairs with G+1 and A-1 in the ligation junction, respectively. (B) Each truncation variant contained a deletion of 6, 9, 12 or 15 nucleotides in the region from A12 to T26. The results showed that residues from T15 to T26 could be deleted without significantly affecting the reaction yield. The ligation reactions were performed in a reaction buffer containing 70 mM Tris (pH 7.5), 1 mM ZnCl₂, 150 mM NaCl and 2 mM KCl at 23°C for 3 h. [Left RNA substrate] = 100 nM. [Right RNA substrate] = 1,000 nM. [Enzyme] = 400 nM. (C) The predicted secondary structures of the full-length deoxyribozyme 7CX10 and the truncated 7CX10t, with RNA substrates, by RNAstructure.

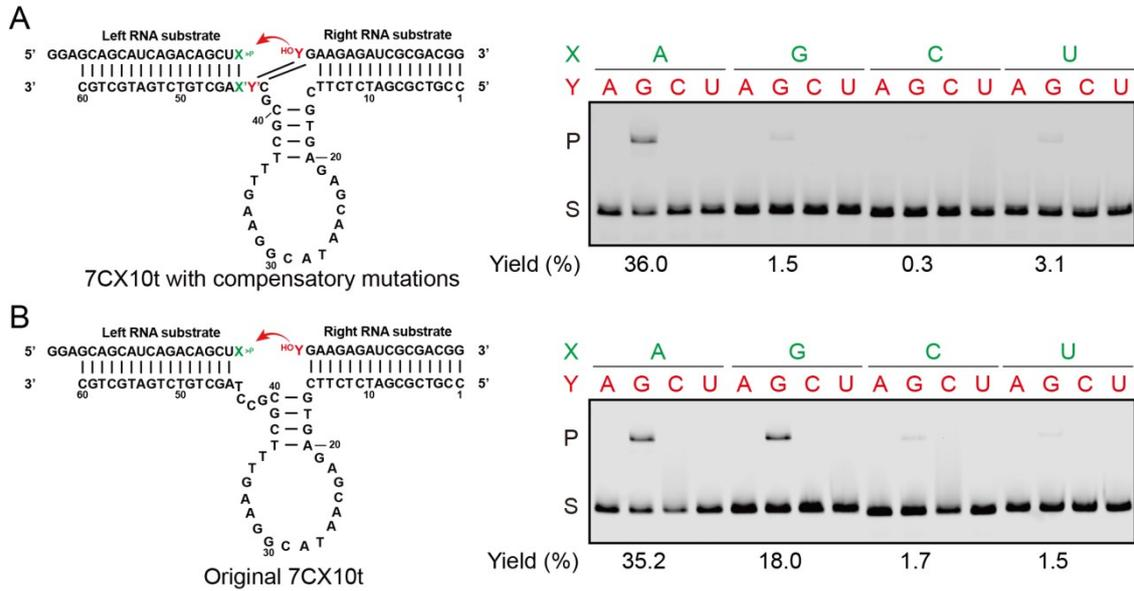


Figure S3. PAGE analysis of 7CX10t-catalyzed ligation of RNA substrates containing 16 different ligation site dinucleotide junctions. (A) Nucleotides (X' and Y') at positions 44 and 43 of 7CX10t were predicted to form base pairs with residues (X and Y) at the ligation site, respectively. For each substrate combination, a corresponding deoxyribozyme 7CX10t variant with compensatory mutations was used. (B) The original deoxyribozyme 7CX10t was used for all the substrate combinations. The ligation reaction was performed in the same buffer at 23°C for 3 h. [Left RNA substrate] = 100 nM. [Right RNA substrate] = 1,000 nM. [Enzyme] = 400 nM.

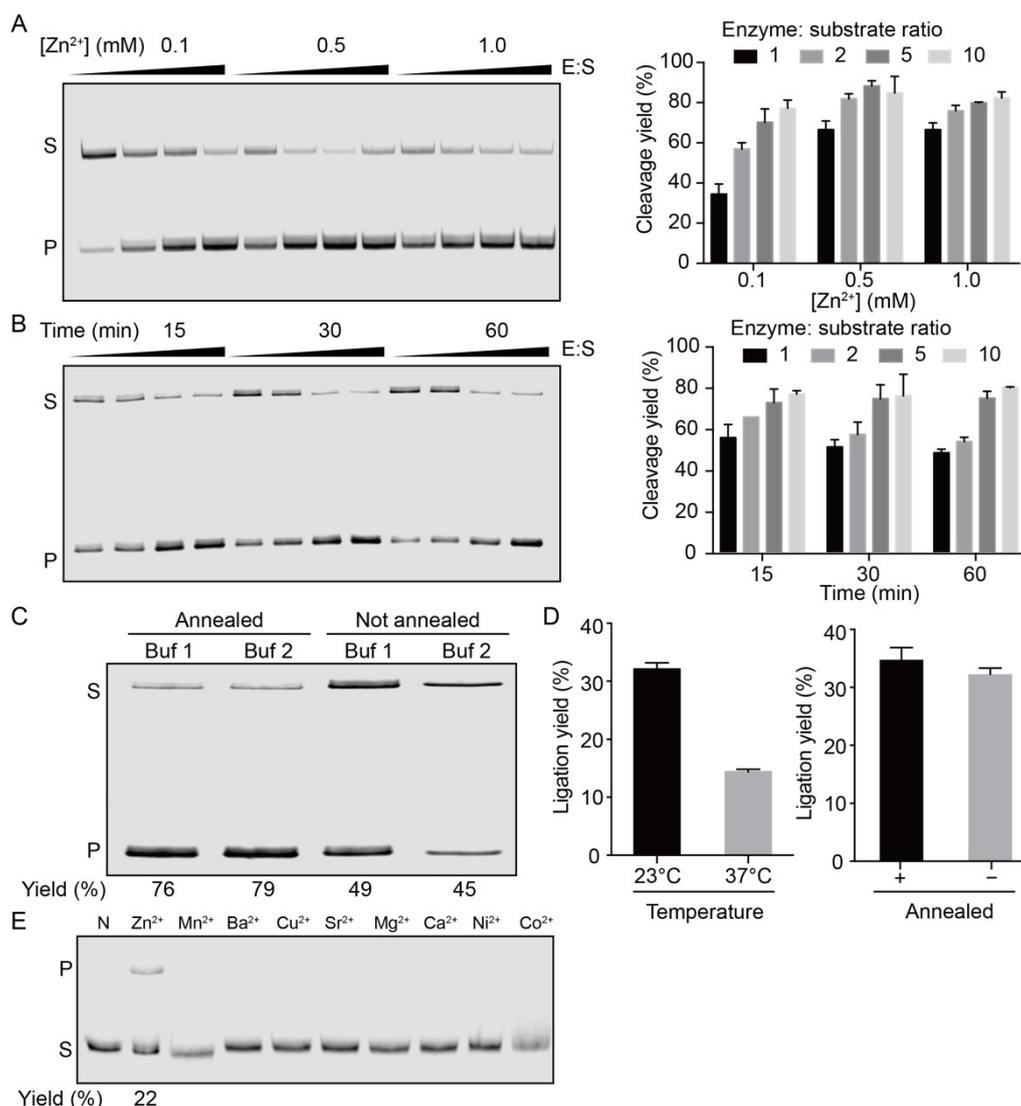


Figure S4. Optimization of the cleavage and ligation reaction conditions. (A) Effects of Zn²⁺ concentration and enzyme:substrate ratio on the 8-17-catalyzed RNA cleavage reaction. The reactions were performed in a buffer containing 50 mM Tris (pH 7.5) and 1 M NaCl at 37°C for 30 min. [Substrate] = 100 nM. The Zn²⁺ and enzyme concentration varied. [Zn²⁺]: 0.1, 0.5 and 1.0 mM. [Enzyme]: 100, 200, 500 and 1,000 nM. (B) Effects of reaction time and enzyme:substrate ratio on the 8-17-catalyzed RNA cleavage reaction. The reactions were performed in a buffer containing 50 mM Tris (pH 7.5), 1 mM Zn²⁺ and 1 M NaCl at 37°C. [Substrate] = 100 nM. The reaction time and enzyme concentration varied. Time: 15, 30 and 60 min. [Enzyme]: 100, 200, 500 and 1,000 nM. (C) Effects of annealing conditions on the 8-17-catalyzed RNA cleavage reaction. Buffer 1 was a typical cleavage reaction buffer of 8-17 containing 50 mM Tris (pH 7.5), 1 mM ZnCl₂ and 1 M NaCl. Buffer 2 was the ligation reaction buffer of 7CX10 containing 70 mM Tris, 1 mM ZnCl₂, 150 mM NaCl and 2 mM KCl at pH 7.5. The results showed that 8-17 was able to catalyze reactions under both buffer conditions with a similar activity. S: substrate. P: cleavage product. (D) Effects of reaction temperature and annealing condition on the ligation reaction. (E) Divalent metal ion dependence of 7CX10t. Divalent metal ion concentration was 10 mM except for Zn²⁺ (1 mM) and Mn²⁺ (1 mM). N: no divalent metal ion.

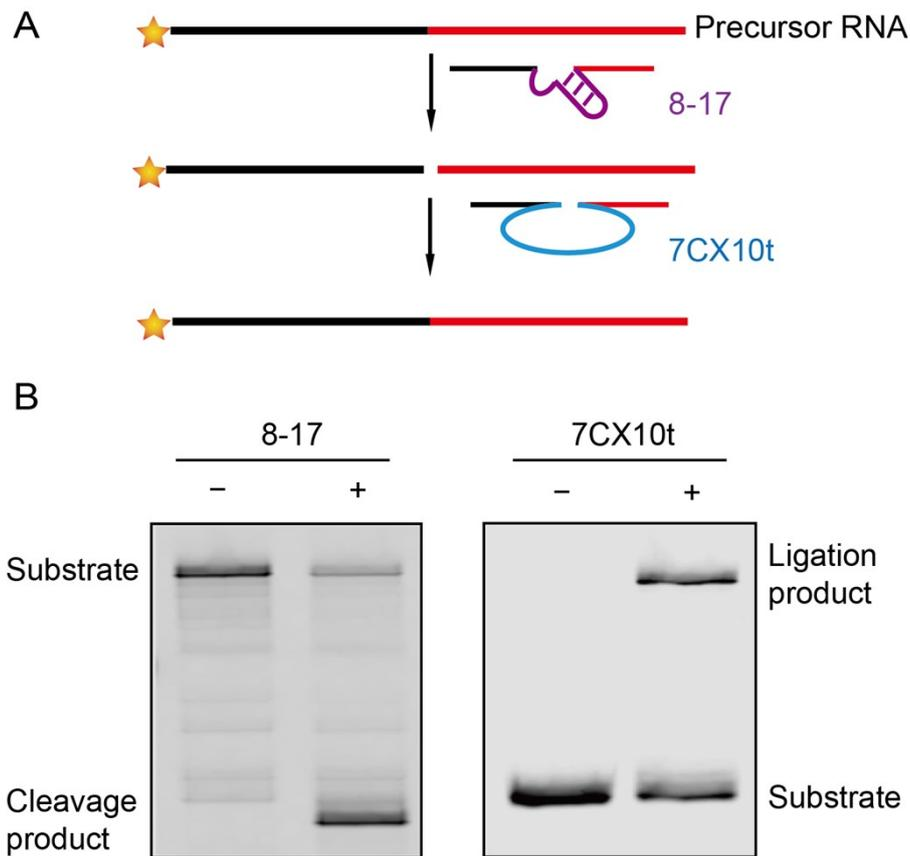


Figure S5. Sequential cleavage and ligation reactions under identical reaction conditions. (A) Schematic diagram of 8-17-catalyzed cleavage reaction and 7CX10t-catalyzed ligation reaction. (B) PAGE analysis of the cleavage and ligation reactions. The cleavage reaction was performed in a reaction buffer containing 70 mM Tris (pH 7.5), 1 mM ZnCl₂, 150 mM NaCl and 2 mM KCl at 23°C for 30 min. [Substrate] = 100 nM. [Enzyme] = 1,000 nM. The ligation reaction was performed in the same buffer at 23°C for 3 h. [Left RNA substrate] = 100 nM. [Right RNA substrate] = 1,000 nM. [Enzyme] = 400 nM.

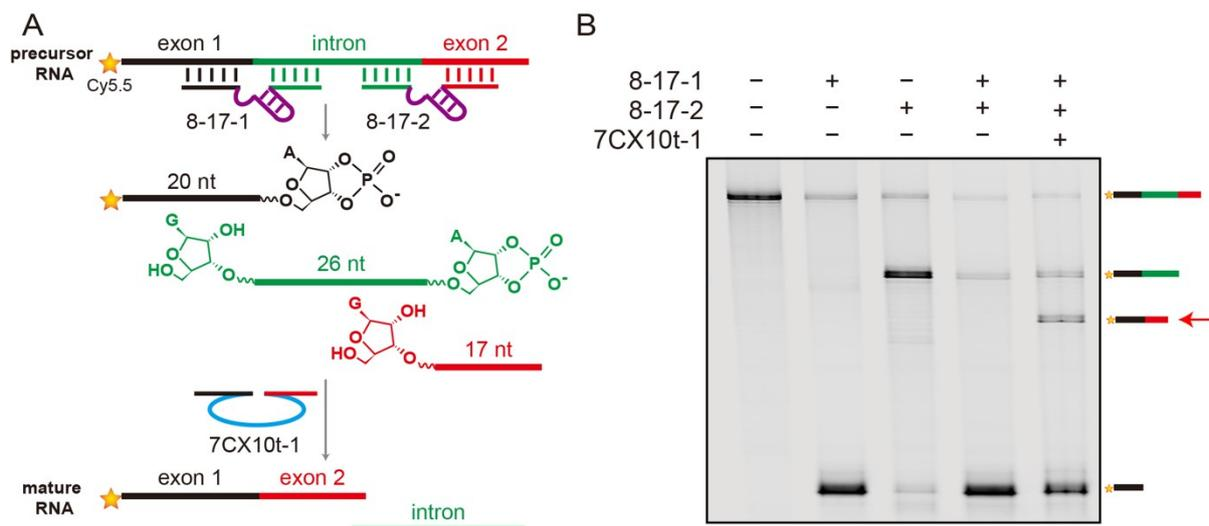


Figure S6. DNA-catalyzed RNA splicing. (a) Schematic representation. Two deoxyribozyme 8-17 variants catalyzed cleavage reactions of the precursor RNA, generating individual fragments of two exons and one intron. Deoxyribozyme 7CX10t then catalyzed RNA ligation reaction, joining two exons together. (b) PAGE analysis of the splicing reactions. Arrow indicates the splicing product.

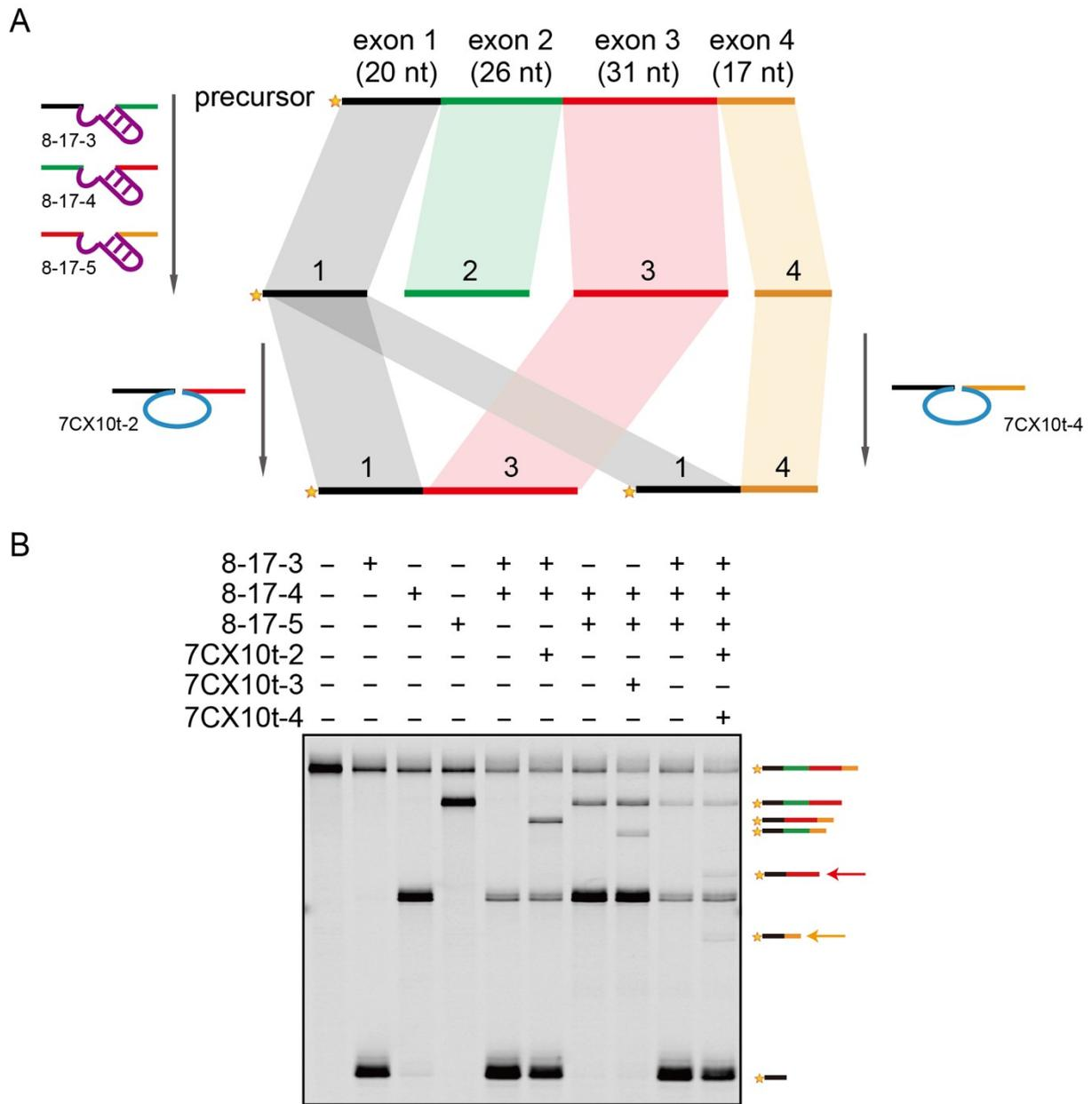


Figure S7. Alternative RNA splicing reactions in one tube generated two different isoforms. (A) Schematic representation. The precursor was first cleaved into four fragments by three 8-17 deoxyribozymes. Two different 7CX10t deoxyribozymes were then used to join together exons 1 and 3, and exons 1 and 4, respectively. (B) PAGE analysis of the alternative RNA splicing reactions in one tube. The last lane showed that in the presence of three 8-17 and two 7CX10t deoxyribozymes, two distinct splicing isoforms could be produced (indicated by red and orange arrows).

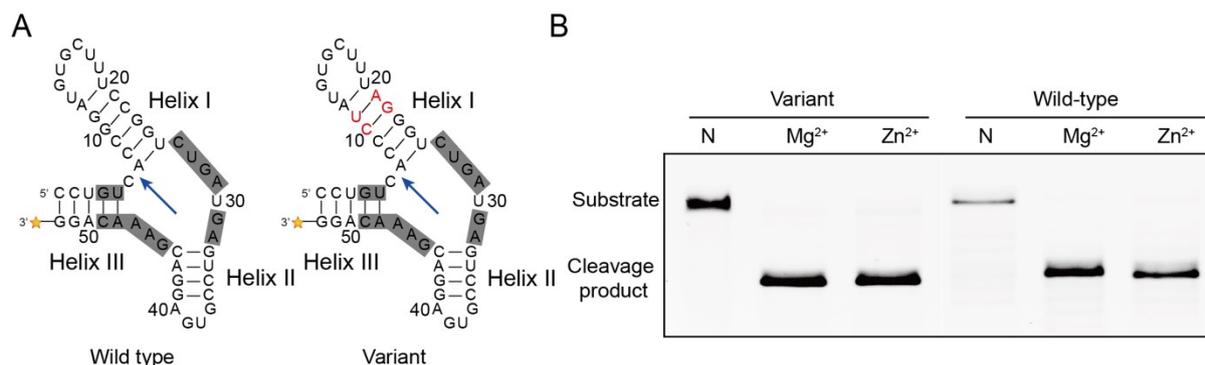


Figure S8. Catalytic activity assay of hammerhead ribozyme wild-type and variant in the presence of different divalent metal ion. (A) The predicted secondary structures of the hammerhead ribozyme wild-type and variant. Substitution of two base pairs (show in red) were introduced in the variant sequence to create a ligation site for deoxyribozyme 7CX10t. Arrows indicate self-cleavage site. Conserved nucleotides at catalytic core region are highlighted. (B) PAGE analysis of the self-cleavage activity of the hammerhead ribozyme wild-type and variant. The reaction was performed in a reaction buffer containing 50 mM Tris (pH 7.0), 10 mM Mg²⁺ or 1 mM Zn²⁺ at 23°C for 10 min. [Ribozyme] = 100 nM. N: no metal ion.

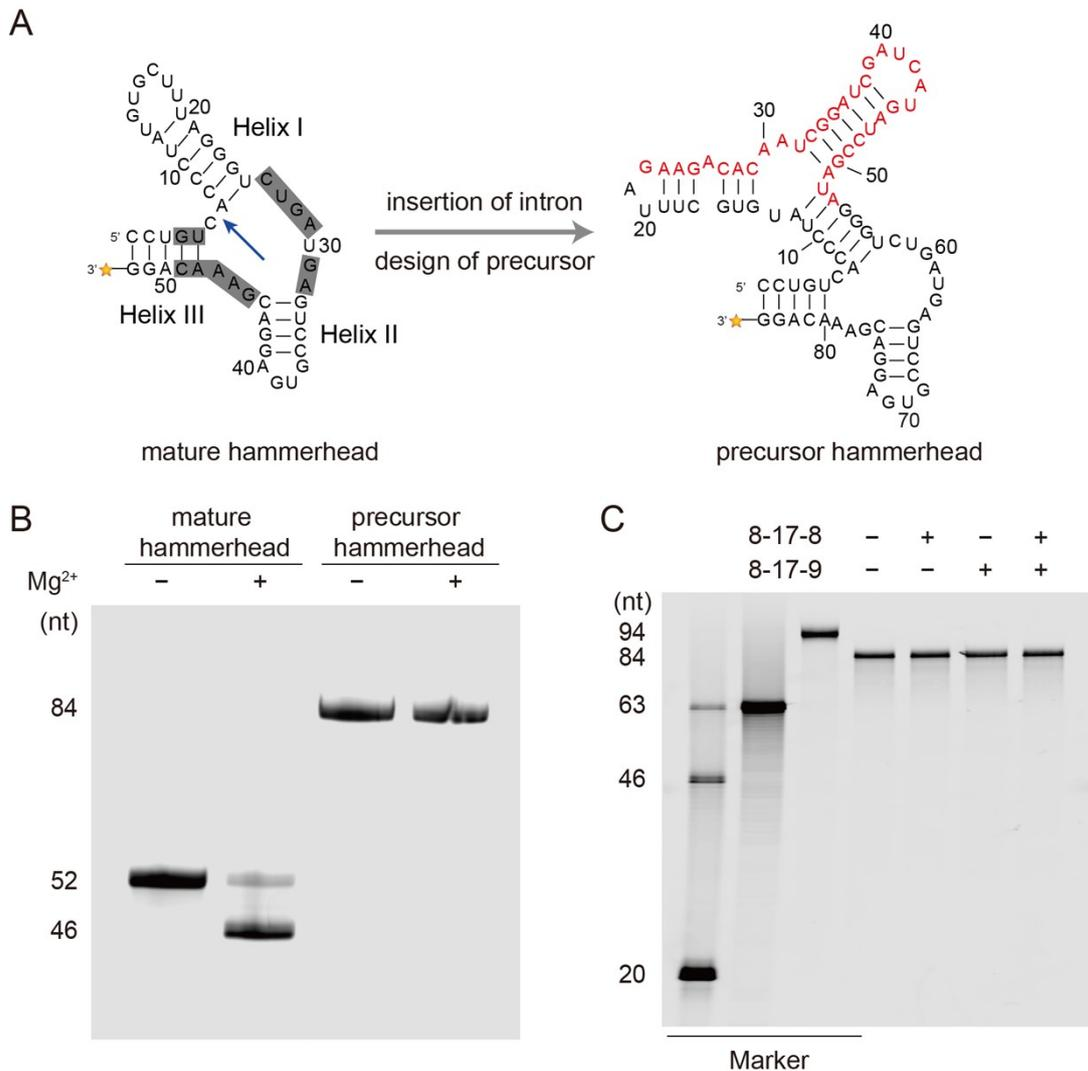


Figure S9. Initial design and activity test of precursor hammerhead ribozyme. (A) The predicted secondary structures of the mature hammerhead ribozyme variant and the initially designed precursor RNA. Intron (shown in red) was introduced into the Helix I region to disrupt correct folding and to block self-cleavage activity of the hammerhead ribozyme. Arrows indicate self-cleavage site. Conserved nucleotides at catalytic core region are highlighted. (B) PAGE analysis of the self-cleavage reactions of the hammerhead ribozyme variant and the initially designed precursor RNA. (C) PAGE analysis of 8-17-catalyzed cleavage reactions of the initially designed precursor RNA. Lanes 1-3 are RNA markers.

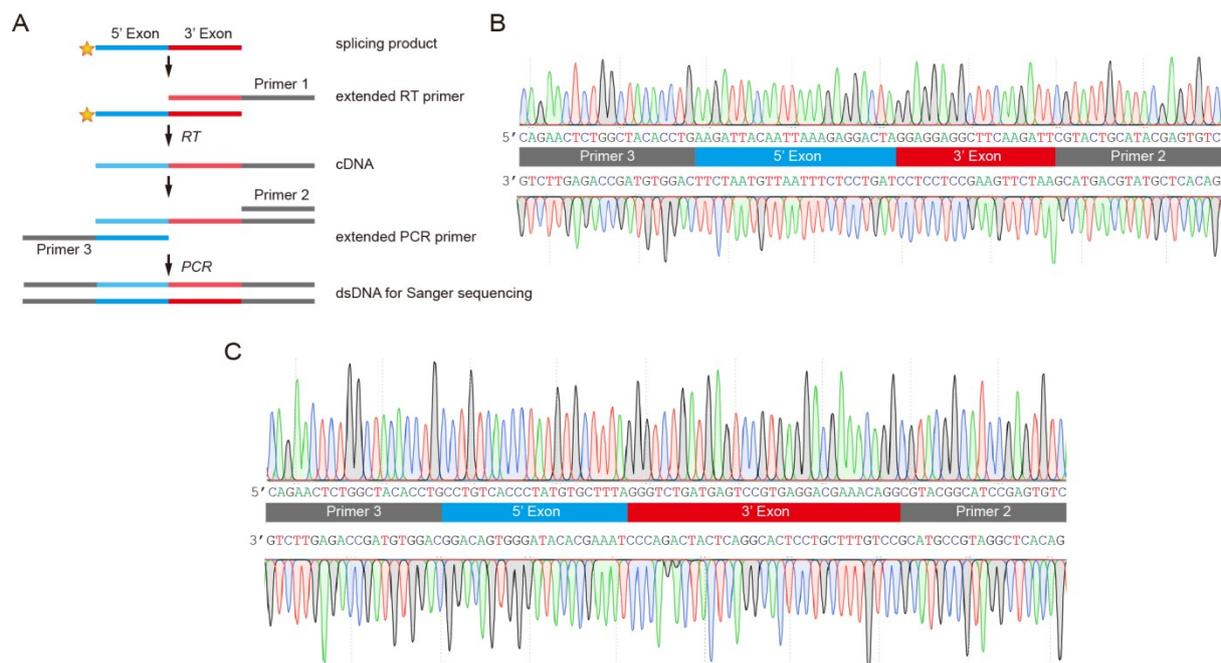


Figure S10. Sequencing analysis of the splicing products G-quadruplex and hammerhead ribozyme variant. (A) Design of sequencing methods. Splicing product RNA was isolated from the DNA-catalyzed splicing reactions and reverse transcribed to generate complementary DNA (cDNA). The cDNA was amplified by PCR, and the amplification products were sent for Sanger sequencing. Lines of the same colour denote complementarity. (B) Sequencing result of the splicing product G-quadruplex. (C) Sequencing result of the splicing product hammerhead ribozyme variant.

Table S1. DNA sequences used in the 7CX10 truncation experiments. The sequences of two substrate-binding arms were omitted and only the central catalytic core region was shown. The conserved regions were highlighted in green. Deletions were shown as red hyphens and were added for alignment purpose.

Name	Sequence (5'->3')
Δ(A9-T11)	GTGAGAGC---ACGTATGAAGATATTGAAGTTTCGCGCCT
Δ(A12-G14)	GTGAGAGCAAT---TATGAAGATATTGAAGTTTCGCGCCT
Δ(T15-T17)	GTGAGAGCAATACG---GAAGATATTGAAGTTTCGCGCCT
Δ(G18-A20)	GTGAGAGCAATACGTAT---GATATTGAAGTTTCGCGCCT
Δ(G21-T23)	GTGAGAGCAATACGTATGAA---ATTGAAGTTTCGCGCCT
Δ(A24-T26)	GTGAGAGCAATACGTATGAAGAT---GAAGTTTCGCGCCT
Δ(G27-A29)	GTGAGAGCAATACGTATGAAGATATT---GTTTCGCGCCT
Δ(G30-T32)	GTGAGAGCAATACGTATGAAGATATTGAA---TCGCGCCT
Δ(T31-T33)	GTGAGAGCAATACGTATGAAGATATTGAAG---CGCGCCT
C39A/T40A	GTGAGAGCAATACGTATGAAGATATTGAAGTTTCGCGCAA
Δ(A12-T17)	GTGAGAGCAAT-----GAAGATATTGAAGTTTCGCGCCT
Δ(T15-A20)	GTGAGAGCAATACG-----GATATTGAAGTTTCGCGCCT
Δ(G18-T23)	GTGAGAGCAATACGTAT-----ATTGAAGTTTCGCGCCT
Δ(G21-T26)	GTGAGAGCAATACGTATGAA-----GAAGTTTCGCGCCT
Δ(A12-A20)	GTGAGAGCAAT-----GATATTGAAGTTTCGCGCCT
Δ(T15-T23)	GTGAGAGCAATACG-----ATTGAAGTTTCGCGCCT
Δ(G18-T26)	GTGAGAGCAATACGTAT-----GAAGTTTCGCGCCT
Δ(A12-T23)	GTGAGAGCAAT-----ATTGAAGTTTCGCGCCT
Δ(T15-T26)	GTGAGAGCAATACG-----GAAGTTTCGCGCCT
Δ(A12-T26)	GTGAGAGCAAT-----GAAGTTTCGCGCCT

Table S2. Summary of the reaction yields. In cleavage reactions where multiple 8-17 deoxyribozymes were present, two reactions yields were calculated. ^a: reaction yield accounting for all the cleavage products. ^b: reaction yield of the cleavage product, typically the 5' fragment, which would be joined in the subsequent ligation reaction.

Deoxyribozyme/Ribozyme	Yield (%)
Sequential cleavage and ligation reactions	
8-17	79.6 ± 0.3
7CX10t	37.1 ± 8.4
Model splicing reaction	
8-17-1	81.1 ± 9.1
8-17-2	78.0 ± 6.7
8-17-1 + 8-17-2	(96.9 ± 2.1) ^a ; (87.2 ± 4.9) ^b
8-17-1 + 8-17-2 + 7CX10t-1	14.6 ± 0.7
Model alternative splicing reaction	
8-17-3	72.5 ± 2.2
8-17-4	71.6 ± 3.0
8-17-5	75.1 ± 2.4
8-17-3 + 8-17-4	(86.0 ± 3.6) ^a ; (74.7 ± 5.0) ^b
8-17-3 + 8-17-4 + 7CX10t-2	17.6 ± 1.5
8-17-4 + 8-17-5	(87.4 ± 3.8) ^a ; (75.1 ± 3.0) ^b
8-17-4 + 8-17-5 + 7CX10t-3	5.7 ± 0.6
8-17-3 + 8-17-4 + 8-17-5	(90.9 ± 4.0) ^a ; (77.4 ± 3.7) ^b
8-17-3 + 8-17-4 + 8-17-5 + 7CX10t-2	3.9 ± 0.9
8-17-3 + 8-17-4 + 8-17-5 + 7CX10t-4	4.0 ± 1.8
G quadruplex splicing reaction	
8-17-6	66.9 ± 4.8
8-17-7	84.6 ± 0.6
8-17-6 + 8-17-7	(88.4 ± 4.8) ^a ; (71.7 ± 4.8) ^b
8-17-6 + 8-17-7 + 7CX10t-5	22.3 ± 3.4
Hammerhead ribozyme splicing reaction	
8-17-8	61.4 ± 2.4
8-17-9	40.7 ± 2.4
8-17-8 + 8-17-9	(75.4 ± 0.9) ^a ; (70.6 ± 3.3) ^b
8-17-8 + 8-17-9 + 7CX10t-6	25.8 ± 1.2
Hammerhead ribozyme self-cleavage reaction	
Chemically synthesized control	86.3 ± 3.1
Precursor RNA	52.4 ± 4.2
Splicing product	75.3 ± 2.0
G4 peroxidase and Broccoli aptamer alternative splicing reaction	
8-17-10	71.9 ± 1.6
8-17-11	36.4 ± 5.0
8-17-12	77.8 ± 4.5

8-17-10 + 8-17-11 + 8-17-12	$(97.5 \pm 0.2)^a$; $(82.4 \pm 0.7)^b$
8-17-10 + 8-17-11 + 8-17-12 + 7CX10t-7	10.5 ± 0.4
8-17-10 + 8-17-11 + 8-17-12 + 7CX10t-8	10.2 ± 0.3

Table S3. Nucleic acid sequences used in the splicing experiments. DNA and RNA sequences were shown in black and red, respectively. The “>p” at the end of the sequence indicates a 2',3'-cyclic phosphate group. Binding arm regions within deoxyribozymes are underlined.

Name	Sequence (5'→3')
Sequential cleavage and ligation reactions	
Full-length RNA	Cy5.5-GGAGCAGCAUCAGACAGCUAGGAAGAGAUCGCGACGG
Left RNA substrate	Cy5.5-GGAGCAGCAUCAGACAGCUA>p
Right RNA substrate	GGAAGAGAUCGCGACGG
8-17	<u>CTCTTCTGTCAGCGACTCGAAAGCTGTC</u>
7CX10t	<u>CCGTCGCGATCTCTTCGTGAGAGCAATACGGAAGTTTCGCGCC</u> <u>TAGCTGTCTGATGCTGC</u>
7CX10t ligation site preference	
RNA substrate-A	Cy5-GGAGCAGCAUCAGACAGCUAGGAAGAGAUCGCGACGG
RNA substrate-G	Cy5-GGAGCAGCAUCAGACAGCUGGGAAGAGAUCGCGACGG
RNA substrate-C	Cy5-GGAGCAGCAUCAGACAGCUCGGAAGAGAUCGCGACGG
RNA substrate-U	Cy5-GGAGCAGCAUCAGACAGCUUGGAAGAGAUCGCGACGG
Universal 8-17	<u>CTCTTCTTCCAGCGGATCGAAAGCTGTC</u>
Right RNA substrate-A	AGAAGAGAUCGCGACGG
Right RNA substrate-G	GGAAGAGAUCGCGACGG
Right RNA substrate-C	CGAAGAGAUCGCGACGG
Right RNA substrate-U	UGAAGAGAUCGCGACGG
7CX10-AA	<u>CCGTCGCGATCTCTTCGTGAGAGCAATACGGAAGTTTCGCGCTT</u> <u>AGCTGTCTGATGCTGC</u>
7CX10-AG	<u>CCGTCGCGATCTCTTCGTGAGAGCAATACGGAAGTTTCGCGCC</u> <u>TAGCTGTCTGATGCTGC</u>
7CX10-AC	<u>CCGTCGCGATCTCTTCGTGAGAGCAATACGGAAGTTTCGCGCG</u> <u>TAGCTGTCTGATGCTGC</u>
7CX10-AU	<u>CCGTCGCGATCTCTTCGTGAGAGCAATACGGAAGTTTCGCGCA</u> <u>TAGCTGTCTGATGCTGC</u>
7CX10-GA	<u>CCGTCGCGATCTCTTCGTGAGAGCAATACGGAAGTTTCGCGCT</u> <u>CAGCTGTCTGATGCTGC</u>
7CX10-GG	<u>CCGTCGCGATCTCTTCGTGAGAGCAATACGGAAGTTTCGCGCC</u> <u>CAGCTGTCTGATGCTGC</u>

7CX10-GC	<u>CCGTCGCGATCTCTTCGTGAGAGCAATACGGAAGTTTCGCGCG</u> <u>CAGCTGTCTGATGCTGC</u>
7CX10-GU	<u>CCGTCGCGATCTCTTCGTGAGAGCAATACGGAAGTTTCGCGCA</u> <u>CAGCTGTCTGATGCTGC</u>
7CX10-CA	<u>CCGTCGCGATCTCTTCGTGAGAGCAATACGGAAGTTTCGCGCT</u> <u>GAGCTGTCTGATGCTGC</u>
7CX10-CG	<u>CCGTCGCGATCTCTTCGTGAGAGCAATACGGAAGTTTCGCGCC</u> <u>GAGCTGTCTGATGCTGC</u>
7CX10-CC	<u>CCGTCGCGATCTCTTCGTGAGAGCAATACGGAAGTTTCGCGCG</u> <u>GAGCTGTCTGATGCTGC</u>
7CX10-CU	<u>CCGTCGCGATCTCTTCGTGAGAGCAATACGGAAGTTTCGCGCA</u> <u>GAGCTGTCTGATGCTGC</u>
7CX10-UA	<u>CCGTCGCGATCTCTTCGTGAGAGCAATACGGAAGTTTCGCGCT</u> <u>AAGCTGTCTGATGCTGC</u>
7CX10-UG	<u>CCGTCGCGATCTCTTCGTGAGAGCAATACGGAAGTTTCGCGCC</u> <u>AAGCTGTCTGATGCTGC</u>
7CX10-UC	<u>CCGTCGCGATCTCTTCGTGAGAGCAATACGGAAGTTTCGCGCG</u> <u>AAGCTGTCTGATGCTGC</u>
7CX10-UU	<u>CCGTCGCGATCTCTTCGTGAGAGCAATACGGAAGTTTCGCGCA</u> <u>AAGCTGTCTGATGCTGC</u>

Model splicing reaction

Precursor RNA	Cy5.5- GGAGCAGCAUCAGACAGCUAGGAAGAGAAGGAGAUUAUUAUAG GCAUAGGAAGAGAUCGCGACGG
8-17-1	<u>TTCTCTTCTGTCAGCGACTCGAAAGCTGTCTG</u>
8-17-2	<u>ATCTCTTCTGTCAGCGACTCGAAATGCCTATA</u>
7CX10t-1	<u>CCGTCGCGATCTCTTCGTGAGAGCAATACGGAAGTTTCGCGCC</u> <u>TAGCTGTCTGATGCTGC</u>

Model alternative splicing reaction

Left RNA fragment	Cy5.5- GGAGCAGCAUCAGACAGCUAGGAAGAGAAGGAGAUUAUUAUAG GCAUAGGAAGAGAUCGCGACGG
Right RNA fragment	phosphate-AAAAUAAUAAAAUAGGUAAAUUUAAGGAGAA
DNA splint	TTTACCTATTTTATTATTTCCGTCGCGATCTCTTCCTATGCCTA TATATCTCCTTCTCTTCCTAGCTGTCTGATGCTGC
Precursor RNA	Cy5.5- GGAGCAGCAUCAGACAGCUAGGAAGAGAAGGAGAUUAUUAUAG GCAUAGGAAGAGAUCGCGACGGAAAAUAAUAAAAUAGGUAA AUUUAAGGAGAA

8-17-3 TCCTTCTCTTCTGTCAGCGACTCGAAAGCTGTCTGATG
8-17-4 GCGATCTCTTCTGTCAGCGACTCGAAATGCCTATATAT
8-17-5 CTCCTTAAATTTACTGTCAGCGACTCGAAATTTTATTATTTCC
7CX10t-2 CCGTCGCGATCTCTTCGTGAGAGCAATACGGAAGTTTCGCGCC
TAGCTGTCTGATGCTGC
7CX10t-3 TTCTCCTTAAATTTACGTGAGAGCAATACGGAAGTTTCGCGCCT
ATGCCTATATATCTCC
7CX10t-4 TTCTCCTTAAATTTACGTGAGAGCAATACGGAAGTTTCGCGCCT
AGCTGTCTGATGCTGC

G quadruplex splicing reaction

Precursor RNA Cy5-AAGAUUACAAUUAAGAGGACUA
GUGCAACUCCGCAGAGACAACAGGAGGAGGCUUCAAGAUU
G quadruplex-
forming RNA AAGAUUACAAUUAAGAGGACUAGGAGGAGGCUUCAAGAUU
control
8-17-6 CGGAGTTGCATGTCAGCGACTCGAAAGTCCTCTT
8-17-7 AGCCTCCTCTGTCAGCGACTCGAAGTTGTCTCT
7CX10t-5 AATCTTGAAGCCTCCTCGTGAGAGCAATACGGAAGTTTCGCGC
CTAGTCCTCTTTAATTGTAA

Hammerhead ribozyme splicing reaction

Left RNA fragment 1 CCUGUCACCCUAUGUGCUUUAGAAGACACAAUCGGAUCGAUC
AUGAUCCGA
Right RNA fragment 1 phosphate-UAGGGUCUGAUGAGUCCGUGAGGACGAAACAGG-
Cy5.5
DNA splint 1 CCTGTTTCGTCCTCACGGACTCATCAGACCCTATCGGATCATGA
TCGATCCGATTGTGTCTTCTAAAGCACATAGGGTGACAGG
Precursor RNA 1 CCUGUCACCCUAUGUGCUUUAGAAGACACAAUCGGAUCGAUC
AUGAUCCGAUAGGGUCUGAUGAGUCCGUGAGGACGAAACAG
G-Cy5.5
Left RNA fragment 2 CCUGUCACCCUAUGUGCUUUAGAAUUAUAAUCGGAUCGAUC
AUGAUCAU
Right RNA fragment 2 phosphate-UAGGGUCUGAUGAGUCCGUGAGGACGAAACAGG-
Cy5.5
DNA splint 2 CCTGTTTCGTCCTCACGGACTCATCAGACCCTAATGATCATGAT
CGATCCGATTATATATTCTAAAGCACATAGGGTGACAGG
Precursor RNA 2 CCUGUCACCCUAUGUGCUUUAGAAUUAUAAUCGGAUCGAUC
AUGAUCAUUAAGGGUCUGAUGAGUCCGUGAGGACGAAACAGG-
Cy5.5
Hammerhead wild-
type CCUGUCACCGGAUGUGCUUUCGGUCUGAUGAGUCCGUGAGG
ACGAAACAGG
Hammerhead variant CCUGUCACCCUAUGUGCUUUAGGGUCUGAUGAGUCCGUGAGG
ACGAAACAGG

8-17-8	<u>GATTGTGTCTTTGTCAGCGACTCGAAAAAGCACATAGG</u>
8-17-9	<u>CTCATCAGACCTGTCAGCGACTCGAAATCGGATCATGA</u>
8-17-10	<u>CCGATTATATATTTGTCAGCGACTCGAAAAAGCACATAGG</u>
8-17-11	<u>CTCATCAGACCTGTCAGCGACTCGAAATGATCATGAT</u>
7CX10t-6	<u>TGTTTCGTCCTCACGGACTCATCAGACCGTGAGAGCAATACGG</u> <u>AAGTTTCGCGCCTAAAGCACATAGGGTGACAGG</u>
<hr/>	
Sequencing of spliced products	
RT primer 1	GACTCTCGTATGCAGTACGAATCTTGAAGCCTCCTCC
G-Primer 2	GACTCTGTATAACAATACG
G-Primer 3	CAGAACTCTGGCTACACCTGAAGATTACAATTAAGAGGACTA
RT primer 2	GACTCTCGTATGCAGTACGCCTGTTTCGTCCTCACGGAC
H-Primer 2	GACTCTGGATGCCGTACG
H-Primer 3	CAGAACTCTGGCTACACCTGCCTGTCACCCTATGTGCTTT
<hr/>	
G4 peroxidase and Broccoli aptamer alternative splicing reaction	
RNA primer	Cy5-GAGACGGUCGGGUCCAGAU
DNA template	GAGCCCACTCTACTCGACAGATATCCTTTTTTTTTTCCCAACC CGCCCTATGTTTCGTGGAGGACTTTAGGTCCTCCTTGATTCTCTA CCCTATATCTGGACCCGACCGTCTC
Precursor RNA	Cy5- GAGACGGUCGGGUCCAGAUUAUAGGGUAGAGAAUCAAGGAGG ACCUAAAGUCCUCCACGAACAUAGGGCGGGUUGGGAAAAAA AAAGGAUAUCUGUCGAGUAGAGUGUGGGCUC
8-17-12	<u>TCCTTGATTCTTGTGTCAGCGACTCGAAACCCTATATCTG</u>
8-17-13	<u>AACCCGCCTGTCAGCGACTCGAAATGTTTCGTGGAG</u>
8-17-14	<u>TACTCGACAGATATCTGTCAGCGACTCGAATTTTTTTTCC</u>
7CX10t-7	<u>TTTTTTTTTCCCAACCCGCCGTGAGAGCAATACGGAAGTTTCGC</u> <u>GCCTACCCTATATCTGGACCCGACCGTCTC</u>
7CX10t-8	<u>GAGCCCACTCTACTCGACAGATATCGTGAGAGCAATACGGA</u> <u>AGTTTCGCGCCTACCCTATATCTGGACCCGACCGTCTC</u>
NC sequence	Cy5.5-GGAGCAGCAUCAGACAGCUAGGAAGAGAUCGCGACGG
<hr/>	

References

1. C. Cozensa, V. B. Pinheiroa, A. Vaismanb, R. Woodgateb and P. Holliger, *Proc. Natl. Acad. Sci. USA*, 2012, **109**, 8067-8072.
2. H.-K. Kim, J. Liu, J. Li, N. Nagraj, M. Li, C. M.-B. Pavot and Y. Lu, *J. Am. Chem. Soc.*, 2007, **129**, 6896-6902.
3. D. M. Kost, J. P. Gerdt, P. I. Pradeepkumar and S. K. Silverman, *Org. Biomol. Chem.*, 2008, **6**, 4391-4398.
4. K. Schlosser, J. Gu, L. Sule and Y. Li, *Nucleic Acids Res.*, 2008, **36**, 1472-1481.
5. R. Hieronymus, J. Zhu and S. Muller, *Nucleic Acids Res.*, 2022, **50**, 368-377.
6. W. Li, Y. Li, Z. Liu, B. Lin, H. Yi, F. Xu, Z. Nie and S. Yao, *Nucleic Acids Res.*, 2016, **44**, 7373-7384.
7. G. S. Filonov, J. D. Moon, N. Svensen and S. R. Jaffrey, *J. Am. Chem. Soc.*, 2014, **136**, 16299-16308.